The Journal of Immunology

Dormant *Mycobacterium tuberculosis* Fails To Block Phagosome Maturation and Shows Unexpected Capacity To Stimulate Specific Human T Lymphocytes

Sabrina Mariotti, Manuela Pardini, Maria Cristina Gagliardi, Raffaela Teloni, Federico Giannoni, Maurizio Fraziano, Francesco Lozupone, Stefania Meschini and Roberto Nisini

J Immunol 2013; 191:274-282; Prepublished online 3 June 2013;
doi: 10.4049/jimmunol.1202900
http://www.jimmunol.org/content/191/1/274

The Journal of Immunology is published twice each month by
The American Association of Immunologists, Inc.,
9650 Rockville Pike, Bethesda, MD 20814-3994.

Print ISSN: 0022-1767 Online ISSN: 1550-6606.

Dormant *Mycobacterium tuberculosis* Fails To Block Phagosome Maturation and Shows Unexpected Capacity To Stimulate Specific Human T Lymphocytes

Sabrina Mariotti,* Manuela Pardini,* Maria Cristina Gagliardi,* Raffaela Teloni,* Federico Giannoni,* Maurizio Fraziano,† Francesco Lozupone,‡ Stefania Meschini,§ and Roberto Nisini*

Dormancy is defined as a stable but reversible nonreplicating state of *Mycobacterium tuberculosis*. It is currently thought that dormant *M. tuberculosis* (D-Mtb) is responsible for latent tuberculosis (TB) infection. Recently, D-Mtb was also shown in sputa of patients with active TB, but the capacity of D-Mtb to stimulate specific immune responses was not investigated. We observed that purified protein derivative–specific human CD4$^+$ T lymphocytes recognize mycobacterial Ags more efficiently when macrophages are infected with D-Mtb instead of replicating *M. tuberculosis* (R-Mtb). The different Ag recognition occurs even when the two forms of mycobacteria equally infect and stimulate macrophages, which secrete the same cytokine pattern and express MHC class I and II molecules at the same levels. However, D-Mtb but not R-Mtb colocalizes with mature phagolysosome marker LAMP-1 and with vacuolar proton ATPase in macrophages. D-Mtb, unlike R-Mtb, is unable to interfere with phagosome pH and does not inhibit the proteolytic efficiency of macrophages. We show that D-Mtb downmodulates the gene *Rv3875* encoding for ESAT-6, which is required by R-Mtb to block phagosome maturation together with *Rv3310* gene product SapM, previously shown to be downregulated in D-Mtb. Thus, our results indicate that D-Mtb cannot escape MHC class II Ag-processing pathway because it lacks the expression of genes required to block the phagosome maturation. Data suggest that switching to dormancy not only represents a mechanism of survival in latent TB infection, but also a *M. tuberculosis* strategy to modulate the immune response in different stages of TB. *The Journal of Immunology*, 2013, 191: 274–282.

Mycobacterium tuberculosis, the etiological agent of tuberculosis (TB), is one of the most successful human pathogens and has acquired the ability to establish latent or progressive infection and persists despite the presence of a fully functioning innate and acquired immune system (1). *M. tuberculosis* may infect susceptible individuals causing primary TB, a usually mild disease that in most cases is controlled by the development of an efficient immune response, even when mycobacteria are not completely cleared (2). Rather, it is supposed that the immune response forces *M. tuberculosis* to shift into a dormant nonreplicating status causing a latent TB infection (LTBI) (3, 4). However, concomitant diseases, acquired immunodeficiencies (5), or treatments with immunosuppressive drugs may facilitate *M. tuberculosis* reactivation (6) causing postprimary TB, a severe disease that has a chronic and often fatal course in the absence of adequate treatment (7).

Despite the mechanisms of immune evasion that *M. tuberculosis* has evolved, a robust immune response may be measured in both active disease and LTBI, with the exception of advanced stages of active diseases that are characterized by anergic T cell responses (8). However, the host immune response may represent a double-edged sword in different TB stages: it has certainly a protective role, but it may also be detrimental to the host and instrumental to *M. tuberculosis* to infect other individuals (9). The immune response also contributes to causing tissue damage, caseum liquefaction (10), and eventually the formation of cavities merging into the bronchial tree. These open lesions permit the communication between TB foci and the external environment, thus making it possible for *M. tuberculosis* to diffuse in the environment by droplets.

In active disease, *M. tuberculosis* mainly infects professional phagocytes in the lungs where it uses strategies such as prevention of phagolysosome maturation, subversion of host cell death pathways, and the immune system to survive and replicate (11, 12). In LTBI, *M. tuberculosis* is thought to survive in a dormant, nonreplicating form supposedly confined in storage cells in lung and other organs (13, 14) of asymptomatic individuals, where it may persist for years. Dormant *M. tuberculosis* (D-Mtb) may be cultured in vitro where it has been shown to be resistant to adverse conditions, as it survives high hypoxia or nutrient deprivation (15, 16). D-Mtb undergoes extensive transcriptional changes that are triggered by hypoxia and a variety of other conditions including environmental cues through the DevR transcription factor. The

*Dipartimento di Malattie Infettive, Parassitarie e Immunomediate, Istituto Superiore di Sanità, 00161 Rome, Italy; †Dipartimento di Biologia, Università di Roma Tor Vergata, 00133 Rome, Italy; ‡Dipartimento del Farmaco, Istituto Superiore di Sanità, 00161 Rome, Italy; and §Dipartimento Tecnologie e Salute, Istituto Superiore di Sanità, 00161 Rome, Italy

Received for publication October 18, 2012. Accepted for publication April 30, 2013.

This work was partially supported by the Seventh Framework Programme of the European Commission "Discovery and Preclinical Development of New Vaccine Candidates for Tuberculosis (NEWTBVAC)" Grant 241745 and by the Italian Program of AIDS Research.

Address correspondence and reprint requests to Dr. Roberto Nisini, Dipartimento di Malattie Infettive, Parassitarie e Immunomediate, Istituto Superiore di Sanità, Viale Regina Elena 299, 00161 Rome, Italy. E-mail address: roberto.nisini@iss.it

The online version of this article contains supplemental material.

Abbreviations used in this article: BCG, bacillus Calmette–Guérin; CM, complete medium; DC, dendritic cell; D-Mtb, dormant *Mycobacterium tuberculosis*; DQ-BSA, dye-quenched BSA; HK, heat-killed; LTBI, latent tuberculosis infection; MOI, multiplicity of infection; o/n, overnight; PPD, purified protein derivative; R-Mtb, replicating *M. tuberculosis*; TB, tuberculosis; TCC, T cell clone; vATPase, vacuolar ATPase.

www.jimmunol.org/cgi/doi/10.4049/jimmunol.1202900

DevR transcription factor controls the upregulation of a subset of genes with a wide variety of functions, including general protection, lipid metabolism, and anaerobic respiration (17). The shift to dormancy is also associated to downregulation of a variety of genes that could, in principle, affect its immunogenicity or capacity to escape immune recognition (18).

Interestingly, morphologic and transcriptome analysis of *M. tuberculosis* in sputum of infected individuals revealed the presence of high percentages of D-Mtb in active TB (19). Moreover, a resuscitation-promoting factor–dependent population of *M. tuberculosis* was recently observed in clinical TB samples, providing further evidence of the presence of D-Mtb in sputa (20). Because sputa of infecting individuals are likely to reflect the population of bacilli present in open TB lung lesions (19), these data suggest that a large population of D-Mtb can be found in active TB lesions and that dormant bacteria are not necessarily only associated to latency. The analysis of the *M. tuberculosis* population in sputa also supports the hypothesis that D-Mtb may be transmitted to susceptible individuals through the infecting droplets released from patients with active TB. To date, no data are available on the interactions of D-Mtb with the immune system. Such interactions could have important functional consequences not only in latent infections, but also in primary and postprimary TB. In this study we monitored the consequence of macrophage infection by D-Mtb or replicating *M. tuberculosis* (R-Mtb) and the resulting Ag-specific T cell activation.

Materials and Methods

Reagents

RPMI 1640 (Euroclone, Devon, U.K.) was used supplemented with 1 mM L-glutamine, 1 mM sodium pyruvate, 1% nonessential amino acids, and 10% FBS (Hyclone, Logan, UT) (complete medium, CM).

M-CSF, GM-CSF, recombinant human IL-4, and recombinant human IL-2 were purchased from R&D Systems (Minneapolis, MN). LPS from *Escherichia coli* 055:B5, BSA chloroquine, methylene blue, and propidium iodide were purchased from Sigma-Aldrich (St. Louis, MO), and bafilomycin A1 was from Santa Cruz Biotechnology (Santa Cruz, CA). Recombinant MP65 was a gift of Dr. R. La Valle, purified protein derivative (PPD) was from Statens Serum Institut (Copenhagen, Denmark), LysoTracker Red DND-99 and probe dye-quenched BSA (DQ-BSA) were from Molecular Probes, auramine was from Becton Dickinson, PHA (HA-16) was from Murex Diagnostics, and the Bio-Rad protein assay kit was from Bio-Rad (Hercules, CA).

Growth of mycobacteria

M. tuberculosis H37Rv (ATCC 27294) was used for all experiments. Aerobic bacteria were grown in agitation in Dubos Tween-albumin broth (Difco, Detroit, MI) and collected at the midlog phase, that is, OD_{600} of 0.4. D-Mtb was generated as previously described (21–23). Briefly, hypoxic bacteria were grown by stirring (120 rpm) in sealed glass tubes containing Dubos Tween-albumin broth and incubated for 25 d at 37°C. This stage corresponds to late nonreplicating persistence phase 2, after the induction of the dormancy regulon and the enduring hypoxic response gene subsets (17, 21). Control tubes with 1.5 μg/ml methylene blue as an indicator of oxygen depletion were included. The cultures were centrifuged at 3000 rpm for 30 min, washed three times in RPMI 1640, and resuspended in RPMI 1640 containing 10% FBS, and aliquots of both forms of *M. tuberculosis* were immediately frozen at −80°C until use. To infect cells with the same number of D-Mtb and R-Mtb, two aliquots of both mycobacteria were then thawed and CFU counts were performed in agar plates. Briefly, determination of bacterial CFU was performed by plating serial dilution of D-Mtb or R-Mtb aliquots on Middlebrook 7H10 agar (Difco) supplemented with 10% oleic acid-albumin-dextrose-catalase enrichment (Difco). Colonies were counted after 21 d of growth at 37°C and 5% CO_2. This procedure allows us to define the number of mycobacteria in the respective aliquots with the best accuracy provided by currently available methods. In fact, samples of both D-Mtb and R-Mtb prepared for 3:1 multiplicity of infection (MOI) were shown to contain comparable amounts of total DNA (measured by quantitative PCR using 16S specific primers), and the protein content measured by colorimetric Bradford assay (Bio-Rad) on equivalent CFU counts of D-Mtb and R-Mtb indicated a slightly reduced protein content in extracts from D-Mtb compared with R-Mtb, and thus the presence of noncountable dead mycobacteria in D-Mtb preparations could be excluded. As a consequence, all the infection experiments were performed at the indicated MOI using aliquots containing comparable amounts of viable mycobacteria. For some experiments, both R-Mtb and D-Mtb were heat-killed (HK) at 80°C for 1 h. All *M. tuberculosis* preparations were analyzed for LPS contamination by the *Limulus* lysate assay (BioWhittaker, Verviers, Belgium) and contained <10 pg/ml LPS.

RNA extraction and quantitative RT-PCR

Bacterial cultures were centrifuged and pellets resuspended in TRIzol reagent (Invitrogen, Carlsbad, CA), transferred to a new tube containing 500 μl 0.1 mm zirconia/silica beads (BioSpec Products, Bartlesville, OK), and passed through six cycles of 50 s each at maximum speed using a Mini-Beadbeater-8 (BioSpec Products). Total RNA was then purified with an SV Total RNA Isolation System (Promega, Madison, WI) and DNase treated before reverse transcription in a final volume of 20 μl using 1 μl ImProm-II reverse transcriptase (Promega) in ImProm-II reaction buffer containing 0.5 mM 2′-deoxynucleoside 5′-triphosphate and 3 mM $MgCl_2$. Quantitative real-time PCR from D-Mtb cDNA was performed in an iCycler iQ (Bio-Rad) with iQ SYBR Green Supermix (Bio-Rad) and 500 nM each primer for 40 cycles as follows: 40 s at 95°C, 40 s at 59°C, and 50 s at 72°C for 40 cycles. Primer sequences were previously described (21). Data were expressed according to the ΔΔCt method by using day 3 cDNA as the reference time point. All reactions were performed in triplicate, and all RNAs were tested for the absence of genomic DNA contamination using quantitative PCR.

Monocyte isolation, macrophage and dendritic cell generation, and infection

This study was approved by the Istituto Superiore di Sanità Review Board, and written informed consent was obtained by the healthy volunteers who participated in the study. PBMC from healthy donors were isolated by Ficoll density gradient. Monocytes were then positively sorted using anti-CD14–labeled magnetic beads (MACS; Miltenyi Biotec, Bergisch Gladbach, Germany) and resuspended in RPMI 1640–based CM. Macrophages and dendritic cells (DC) were generated culturing monocytes in CM containing 50 ng/ml M-CSF for 6 d or 50 ng/ml GM-CSF and 1000 U/ml IL-4 for 5 d, respectively (24). Differentiated cells were infected with *M. tuberculosis* at MOIs ranging from 1:1 to 10:1 and the MOI of 3:1 was used unless otherwise indicated for overnight (o/n) incubation. In some experiments, HK mycobacteria were used to treat macrophages at the ratio of 3:1. Where indicated, LPS at 0.1 μg/ml was added as positive control the sixth day of culture to induce macrophage or DC activation.

The viability of macrophages and DC after infection with D-Mtb or R-Mtb was evaluated by flow cytometry using the Live/Dead fixable dead cell stain kits (Invitrogen), an assay based on the reaction of a fluorescent-reactive dye with cellular amines. Cells were infected (MOI of 1:1 and 3:1) with bacteria o/n and then incubated up to 3 d. Cells were then stained with fluorescent-reactive dye (0.5 μM, 30 min at room temperature), fixed o/n with 4% paraformaldehyde, and finally analyzed by flow cytometry. No significant difference in viability between D-Mtb– or R-Mtb–infected macrophages or DC was observed in the 3 d of culture.

Phagocytosis assays

Infection of human macrophages with D-Mtb or R-Mtb was assessed by counting intracellular mycobacteria in cells stained with the Kinyoun method, and the efficiency of infection was quantitated by counting the CFU. Macrophages were infected with D-Mtb or R-Mtb (MOI of 1:1) for 1 h and then cultured o/n in the presence of kanamycin (100 U/ml) to kill extracellular mycobacteria. Cells were washed three times using warm RPMI 1640 to remove antibiotics and noninternalized mycobacteria and lysed immediately or after an additional 1, 3, or 6 d culture. Lysis was performed using distilled water containing 0.1% saponin for 5 min at room temperature. For CFU counts, cell lysates were briefly sonicated and 10-fold dilutions were performed using 0.05% Tween 80 in distilled water before plating on Middlebrook 7H10. After 21 d incubation at 37°C in 5% CO_2 atmosphere, CFU in each plate were enumerated.

FACS analysis

Infected APC were collected and stained for 30 min at 4°C with the following mAbs: anti–HLA class I, HLA-DR class II, CD40, CD80, CD83, CD86, and CCR7 or appropriate isotype controls (all from BD Pharmingen). Then, stained cells were fixed o/n with 4% paraformaldehyde and

analyzed using a FACScan cytometer equipped with CellQuest software (Becton Dickinson) acquiring 2×10^4 events gated according to macrophage or DC forward and size scatters.

Staining of acidic vesicles and analysis of proteolytic capacity

LysoTracker Red DND-99 is a fluorescent acidotropic probe that accumulates in lysosomes and is used for the staining and semiquantitative evaluation of acidic intracellular organelles by FACS. Macrophages were infected or treated with viable or HK bacteria, respectively, for 7, 24, or 48 h and then incubated with LysoTracker Red DND-99 probe (0.5 μM, 20 min at 37°C) followed by fixation with 4% paraformaldehyde o/n. Then cells were analyzed by flow cytometry collecting FL2 fluorescence. Untreated and unstained cells and cells treated with bafilomycin A1 (50 nM) were used as controls to set the background fluorescence. To measure by flow cytometry the proteolytic capacity of phagosomes, macrophages were infected or treated with viable or HK bacteria, respectively, for 6, 24, or 72 h and then incubated with DQ-BSA as specified by the manufacturer. Cells treated with chloroquine (50 μM) served as a control to set the background fluorescence. Cells were then fixed with 4% paraformaldehyde o/n and analyzed by flow cytometry collecting FL4 fluorescence.

Confocal microscopy

Monocytes (4×10^5/ml) were allowed to differentiate into macrophages on glass coverslips (12 mm diameter; Thermo Scientific) on the bottom of 12-well plates (Costar). Adherent macrophages were infected with D-Mtb or R-Mtb at an MOI of 1:1 or treated with HK R-Mtb at a ratio of 1:1 and cultured for 6, 24, or 72 h. At the end of the indicated culture period, macrophages were washed in PBS and fixed o/n in 4% (w/v) paraformaldehyde/PBS at room temperature. After washing with PBS, cells were permeabilized in 0.5% (v/v) Triton X-100/PBS for 5 min and washed before treatment with auramine according to the manufacturer's instructions to stain the intracellular *M. tuberculosis*. Cells were washed twice with BSA/PBS and incubated for 2 h at room temperature with diluted LAMP-1 (Santa Cruz Biotechnology) or vacuolar proton ATPase (vATPase) A1 (Santa Cruz Biotechnology) (1:200 in 2% [w/v] BSA/PBS) Abs. After washing with BSA/PBS, the cells were incubated for 1 h at room temperature with 1:100 in PBS Alexa Fluor 488 donkey anti-mouse IgG (Invitrogen, Grand Island, NY) or Alexa Fluor 546 donkey anti-goat IgG (Invitrogen) for LAMP-1 and vATPase, respectively. In some stainings human serum diluted 1:50 was added before staining with the secondary Ab owing to a weak cross-reaction between the Abs used.

For confocal analysis of acidic intracellular organelles, adherent macrophages infected or treated with viable or HK bacteria, respectively, were cultured for 48 h. Macrophages were then washed in PBS and incubated with LysoTracker Red DND-99 (0.5 μM, 20 min at 37°C) before fixation with 4% paraformaldehyde o/n.

After gentle washing with PBS, the coverslips were mounted in buffered 1:1 (v/v) PBS-glycerine solution on prewashed slides.

Confocal laser scanning microscopy analysis was performed by using 488-nm excitation wavelength for direct auramine staining and 549-nm excitation wavelength for LAMP-1, vATPase, or LysoTracker Red DND-99. Emission lines were collected after passage through a DD488/543 filter in a spectral window ranging from 515 to 700 nm. Signals from different fluorescent probes were taken in sequential scan mode, allowing the elimination of channel crosstalk, and colocalization was detected in an overlay model. Images were processed by using LCS software (Leica Microsystems).

Quantitation of colocalization of mycobacteria with LAMP-1 and vATPase was performed by counting the green (noncolocalized) and yellow spotted (colocalized) mycobacteria up to 300 in processed merged images, considering occasional clumps as one *Mycobacterium* when displaying the same color.

Cytokine determination

Supernatants were collected after o/n incubation of APC with mycobacteria and frozen until use. IL-6, IL-8, IL-1β, and TNF-α were measured by ELISA using commercially available kits (R&D Systems Europe). Supernatants from the Ag presentation assays were collected after 48 h culture and evaluated for IFN-γ production by ELISA (R&D Systems Europe). ELISAs were performed according to the manufacturer's instructions, and cytokine levels were expressed in picograms per milliliter. Detection limit of the assays was 15 pg/ml.

Ag-specific human CD4$^+$ T lymphocytes

PPD- and MP65-specific MHC class II–restricted human CD4$^+$ T cell clones (TCC) were isolated from a *Mycobacterium bovis* bacillus Calmette–Guérin (BCG)–vaccinated subject as previously described (24, 25). Clones were restimulated with PHA in the presence of recombinant human IL-2 (R&D Systems) and irradiated PBMC as feeder and cultured for 15–20 d. TCC were then washed twice to remove IL-2, counted, and resuspended in CM. One MP65-specific clone and seven PPD-specific TCC (RNPD3, RNPD36, RNPD49, RNPD50, RNPD73, RNPD130, and RNPD140) were used in this study.

Ag presentation assays

Macrophages or DC isolated from the same donor of TCC were plated into 96-well flat-bottom plates (20×10^3 cells/well) and infected or not with different MOI of D-Mtb or R-Mtb. After o/n incubation, PPD-specific TCC were added (30×10^4 cells/well) and supernatants were examined for IFN-γ production by ELISA after 48 h culture. In some experiments, after o/n incubation, infected and noninfected autologous macrophages were pulsed with 10 μg/ml MP65 for 2 h. Then, an MP65-specific TCC (30×10^4 cells/well) was added and IFN-γ release was measured after 48 h coculture. Where indicated, the macrophages were treated o/n with HK bacteria.

Statistical analysis

All the statistical analyses were performed using the fourth version of GraphPad Prism software. The data were analyzed using the nonparametric Mann–Whitney *U* test. All tests for statistical significance were two-tailed and p values <0.05 were considered significant.

Results

Growth characteristic and capacity to infect human macrophages of D-Mtb and R-Mtb

The growth of D-Mtb, produced in vitro as previously described (21) according to the Wayne model (22, 23), was monitored by OD of the D-Mtb culture. After an initial growth, D-Mtb reached a stationary phase that persisted up to day 40. OD increased during the early phase and was arrested as the conditions became hypoxic, with bacteria entering nonreplicating persistence phase 1 (Fig. 1A). In parallel, *dosR* regulon induction was monitored by RT-PCR. Fig. 1B shows that D-Mtb upregulates α-crystallin (*hspX*) gene expression (26), which peaked around day 9 and dropped to levels characteristic of late nonreplicating persistence phase 2 stages (17) at day 25. In contrast, *esat6* gene expression was progressively downregulated in D-Mtb.

To test whether the different metabolic state of *M. tuberculosis* influences the capacity to infect host cells, macrophages were infected at different MOI of D-Mtb or R-Mtb, and the percentage of infected cells was evaluated after o/n infection as well as the number of infecting mycobacteria after culture in the presence of antibiotics and lysis of macrophages to count the effective numbers of intracellular *M. tuberculosis*. Results indicate that D-Mtb and R-Mtb infect the same percentage of macrophages as measured by phase-contrast light examination after acid-fast Kinyoun staining (Fig. 1C). Moreover, CFU counting of intracellular mycobacteria after overnight infection and lysis of macrophages (Fig. 1D) confirmed that D-Mtb and R-Mtb share the same ability to infect human macrophages. Of note, in the first 6 d after infection D-Mtb remained nonreplicating in infected macrophages (Fig. 1E), confirming previous data obtained with infected THP1 cells (21).

D-Mtb induces the activation of PPD-specific human TCC more efficiently than does R-Mtb

To test the immunogenicity of D-Mtb, we used a set of PPD-specific human CD4$^+$ TCC previously generated from a BCG-vaccinated donor (24) and studied the TCC capacity to proliferate and release IFN-γ in response to autologous macrophages infected with D-Mtb or R-Mtb. From our panel of PPD-specific human CD4$^+$ TCC, we selected seven TCC that were able to recognize Ag when autologous macrophages were infected with BCG. In an initial screening, we noticed that D-Mtb–infected macrophages constantly stimulated specific TCC with higher efficiency than did R-Mtb–infected macrophages (Fig. 2A).

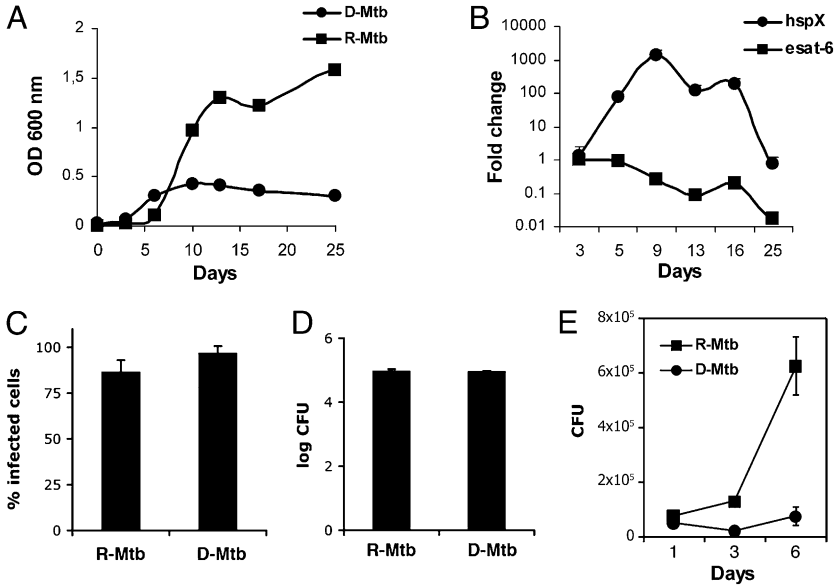

FIGURE 1. Growth characteristic, α-crystallin/ESAT-6 gene expression, and capacity to infect human macrophages of D-Mtb and R-Mtb. (**A**) After an initial growth, D-Mtb reached a stationary phase that persisted up to day 40. All the experiments of Ag presentation were performed using D-Mtb after 25 d culture with the Wayne method. Growth was measured as OD_{600}. (**B**) D-Mtb gene expression of α-crystallin (*hspX*, *Rv2031c*) and *esat6* (*Rv3875*) was determined by quantitative RT-PCR at the indicated intervals. Data are expressed as fold change compared with day 3 mRNA levels. After o/n infection with D-Mtb or R-Mtb at an MOI of 3:1, no differences were observed in the percentages of infected macrophages (**C**) and comparable amounts of bacteria grow after lysis of infected macrophages (**D**). (**E**) D-Mtb does not reactivate in infected macrophages in the first 6 d culture. Macrophages were infected with D-Mtb or R-Mtb (MOI of 1:1) for 1 h and then cultured o/n in the presence of kanamycin (100 U/ml) to kill extracellular mycobacteria. Cells were washed three times using warm RPMI 1640 to remove antibiotics and noninternalized mycobacteria and cultured for 1, 3, or 6 days. For CFU counts, at the end of the indicated culture period, macrophages were lysed using distilled water containing 0.1% saponin for 5 min at room temperature and then plated on Middlebrook 7H10 as specified in *Materials and Methods*. After 21 d incubation at 37°C in 5% CO_2 atmosphere, CFU in each plate were enumerated. (C)–(E) report means ± SEM of data obtained from two independent experiments.

The same result was also obtained using macrophages infected with different MOI of D-Mtb or R-Mtb (Fig. 2B). In fact, at all the MOI tested, D-Mtb–infected macrophages induced a stimulation of specific TCC, measured as IFN-γ secretion, higher than macrophages infected with R-Mtb. The increased capacity of D-Mtb to activate specific T lymphocytes in comparison with R-Mtb was also observed using different APC, such as DC (Fig. 2C). However, because the TCC we used are specific for PPD, which is a complex mixture of *M. tuberculosis* Ags, it is not possible to define the precise epitope recognized by individual clones. Therefore, because we could demonstrate that macrophages are infected with the same efficacy by the two forms of *M. tuberculosis* (Fig. 1C, 1D), the results may indicate that 1) D-Mtb expresses increased amounts of the Ag recognized by our clones in comparison with R-Mtb, 2) the two forms of *M. tuberculosis* induce a different expression of APC stimulatory and costimulatory molecules, or 3) D-Mtb is processed and presented with a higher efficiency than R-Mtb by infected APC.

To test these hypotheses, we first treated the same macrophage population with HK bacteria. As killed bacteria cannot vary the amount of Ag by synthesis or degradation, the activation of TCC is reasonably dependent on the amount of Ag load delivered by dead bacteria into APC. Results clearly show that macrophages treated with HK D-Mtb or HK R-Mtb equally activate TCC (Fig. 2D). Data indicate that 1) the tested TCC recognize epitopes shared by both forms of *M. tuberculosis*, and 2) the recognized peptides derive from the processing of protein Ags expressed at similar amounts in D-Mtb and R-Mtb.

D-Mtb and R-Mtb similarly activate human APC

It is well known that one of the mechanisms developed by *M. tuberculosis* to elude the immune system is by interfering with MHC class II molecule expression and with the activation of infected APC (11). Interestingly, D-Mtb caused a reduction of the MHC class II molecule expression on APC, but the extent of reduction was comparable to that caused by R-Mtb (Fig. 3A–C). Alternatively, neither D-Mtb nor R-Mtb interfered significantly with the expression of MHC class I molecules on APC (data not shown). To test whether infection with D-Mtb or R-Mtb induces different expression of costimulatory molecules on APC, we measured the membrane expression levels of CD80, CD86, and CD40 on macrophages (Fig. 3D) and CD80, CD86, CD83, and CCR7 expression on DC (Fig. 3E). Results indicate that infection with D-Mtb or R-Mtb caused a similar upregulation of the costimulatory molecules on both macrophages and DC. Data suggest that D-Mtb–infected APC do not activate specific TCC with a higher efficiency than do R-Mtb–infected APC as a consequence of an augmented expression of costimulatory molecules. Accordingly, the activation of macrophages and DC following infection with D-Mtb or R-Mtb caused the secretion of comparable amounts of IL-6, IL-8, and TNF-α (Table I). Of note, D-Mtb induced macrophages to secrete significantly lower amounts of IL-1β in comparison with R-Mtb, suggesting that D-Mtb has a reduced capacity to activate macrophage inflammasomes.

D-Mtb does not interfere with the phagosome maturation and the protein processing functions of infected macrophages

One of the earliest virulence traits described for R-Mtb was its ability to block the phagolysosome maturation in infected macrophages. To test whether D-Mtb shares this capacity with R-Mtb, we analyzed phagosome/lysosome fusion in D-Mtb– or R-Mtb–infected human macrophages by confocal laser scanning microscopy. Infected macrophages were stained for the lysosomal marker protein LAMP-1, and *M. tuberculosis* was stained with auramine.

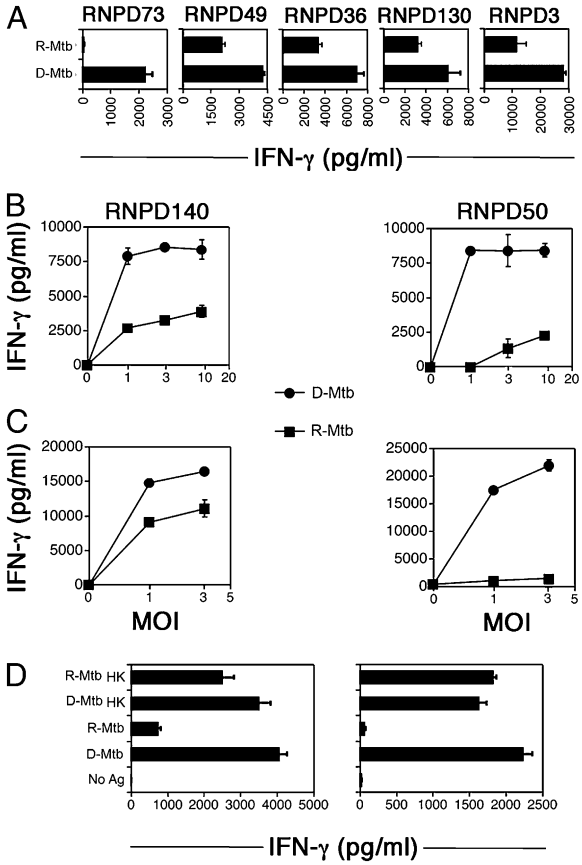

FIGURE 2. D-Mtb is more immunogenic than R-Mtb. Human PPD-specific $CD4^+$ TCC were used to compare the immunogenicity of D-Mtb and R-Mtb. (**A**) Human macrophages were infected o/n with D-Mtb or R-Mtb at an MOI of 3:1 and then cultured with five different autologous PPD-specific $CD4^+$ TCC. One representative experiment out of two is shown. Two additional PPD-specific $CD4^+$ TCC (RNPD140 and RNPD50) were used to measure the MOI-dependent Ag presentation of autologous macrophages (**B**) or DC (**C**) infected o/n with D-Mtb or R-Mtb. One representative experiment out of five is shown. (**D**) Human macrophages were o/n infected with D-Mtb or R-Mtb or treated with the same ratio of HK bacteria and then cultured with two autologous PPD-specific $CD4^+$ TCC (RNPD49 and RNPD73). One representative experiment out of two is shown. Data are expressed as means ± SD of triplicate wells.

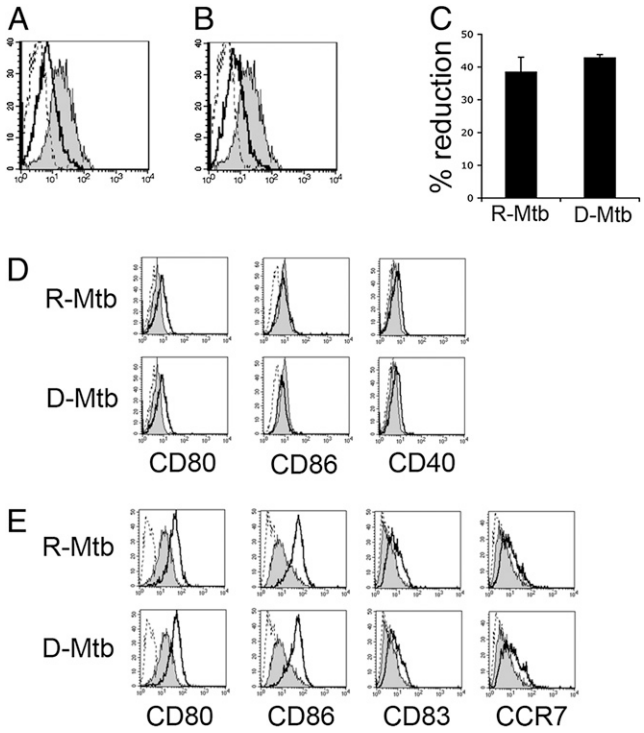

FIGURE 3. D-Mtb– or R-Mtb–infected human APC undergo similar phenotypic modifications. Human macrophages or DC were infected and cultured o/n with D-Mtb or R-Mtb. APC were then stained for surface molecule expression. D-Mtb–infected (**A**) or R-Mtb–infected (**B**) macrophages showed a similar MHC class II downregulation after o/n culture. (**C**) Percentage of MHC class II downregulation in macrophages was similar after infection with D-Mtb or R-Mtb. Data are mean values ± SEM of two independent experiments. Expression is shown of membrane activation markers in infected and noninfected human macrophages (**D**) or DC (**E**) after o/n culture. In (A), (B), (D), and (E), dotted line indicates isotype control, bold line indicates infected cell, and filled curve signifies noninfected cells. One representative experiment out of two is shown.

Confocal microscopy confirmed that both D-Mtb and R-Mtb were internalized by macrophages, because auramine staining was observed in intracellular layers (Fig. 4A) by Z scanning. More interestingly, confocal microscopy showed that most D-Mtb colocalized with LAMP-1, whereas most R-Mtb were found in the LAMP-1^- compartments (Fig. 4A). Some D-Mtb cells were observed to colocalize with LAMP-1 already at 6 h after the infection, and colocalization reached the highest frequency at 24 h after the infection and remained stable at 72 h, when some D-Mtb cell degradation was observed. Most R-Mtb was found in cellular compartments not expressing LAMP-1 at all the tested times (Fig. 4A).

Previous studies showed that R-Mtb is capable of increasing the phagosome pH by mechanisms involving the exclusion of the vATPase from the phagosomal membrane (27). In agreement with previous data, confocal microscopy showed most R-Mtb in compartments where vATPase was excluded (28). Conversely, D-Mtb was found colocalized with vATPase with a frequency that increased in the time course of infection (Fig. 4B) similarly to HK R-Mtb (Supplemental Fig. 1). We then monitored the phagosomal acidity using LysoTracker Red, a dye whose fluorescence measures acidic vesicles (29) by flow cytometry (30) to evaluate the functional consequences of the differential vATPase recruitment in D-Mtb– or R-Mtb–containing phagosomes. As a control, we observed that the fluorescence of LysoTracker Red–stained macrophages was reduced using bafilomycin (27), a specific vATPase inhibitor (not shown). Interestingly, we found that D-Mtb, as well as HK mycobacteria, did not reduce the fluorescence of LysoTracker Red–stained acidic vesicles in infected macrophages (Fig. 5A). Alternatively, R-Mtb reduced the fluorescence of LysoTracker Red (Fig. 5B) with a time-dependent mechanism (Supplemental Fig. 2A). Confocal microscopy (Supplemental Fig. 2B) confirmed data obtained by flow cytometry showing a reduced number of acidic compartments in R-Mtb–infected macrophages, whereas D-Mtb–infected macrophages displayed a LysoTracker Red staining similar to noninfected macrophages, as well as to macrophages treated with HK R-Mtb. Because one of the consequences of vATPase-mediated phagosome acidification is the activation of proteolytic enzymes that can process Ags, we measured the proteolytic capacity of macrophages infected by the two forms of *M. tuberculosis* by means of the probe DQ-BSA, which acquires fluorescence on proteolysis. The fluorescence of noninfected macrophages (Fig. 5C) was reduced using chloroquine, which inhibits the activation of proteolytic enzymes by increasing the phagosomal pH. In agreement with the observed capacity of R-Mtb to increase the phagosomal pH, the mean DQ-BSA–dependent fluorescence of R-Mtb–infected macrophages was re-

Table I. Cytokine secretion after o/n infection of macrophages and DC with D-Mtb or R-Mtb

APC	IL-8		IL-6		IL-1β		TNF-α	
	Macrophages	DC	Macrophages	DC	Macrophages	DC	Macrophages	DC
No stimulus	2059 ± 351	420 ± 23	0	426 ± 15	0	0	0	18 ± 7
LPS	6715 ± 1121	5043 ± 418	651 ± 110	11,322 ± 418	197 ± 24	857 ± 118	2410 ± 672	11,444 ± 180
R-Mtb	4979 ± 981	4986 ± 123	432 ± 71	11,303 ± 107	503 ± 189	413 ± 7	849 ± 104	8,143 ± 507
D-Mtb	5012 ± 878	5114 ± 187	363 ± 82	11,361 ± 149	237 ± 102[a]	371 ± 29	863 ± 69	8,024 ± 349

Cytokine secretion is measured in picograms per milliliter, and data indicate mean values ± SEM of three experiments.
[a] $p < 0.05$ of IL-1β secretion between R-Mtb–infected and D-Mtb–infected macrophages.

duced and dependent on the MOI (Fig. 5D). Conversely, macrophages infected with D-Mtb maintained the same level of fluorescence of noninfected APC, indicating that D-Mtb, as well as HK D-Mtb and HK R-Mtb, did not block proteolysis (Fig. 5C). To confirm the inability of D-Mtb to interfere with Ag processing and presentation, we tested whether D-Mtb– or R-Mtb–infected macrophages differently process a non-*M. tuberculosis*–related soluble protein internalized by endocytosis. Macrophages infected with D-Mtb or R-Mtb or treated with HK bacteria were pulsed with MP65, a recombinant *Candida albicans* protein, and the activation of an MP65-specific T cell clone (31) was used as a readout of the capacity of macrophages to process and present this Ag. Fig. 5E shows that whereas R-Mtb reduced the capacity of infected macrophages to present MP65 to specific T cells in an MOI-dependent manner, D-Mtb did not significantly interfere with the Ag processing and presentation of the protein. In fact, the activation of MP65-specific TCC cultured with D-Mtb–infected macrophages was similar to the activation of TCC stimulated by noninfected APC or by macrophages treated with HK R-Mtb. Taken together, these results suggest that by shifting to dormancy, *M. tuberculosis* may lose the ability to interfere with the protein processing capacity of macrophages, permitting an efficient Ag presentation and T cell activation.

Discussion

In this study we describe a previously underestimated feature of *M. tuberculosis* that, by shifting to dormancy, may allow phagosome maturation, thus favoring the Ag processing in infected macrophages and ultimately its recognition by Ag-specific T lymphocytes.

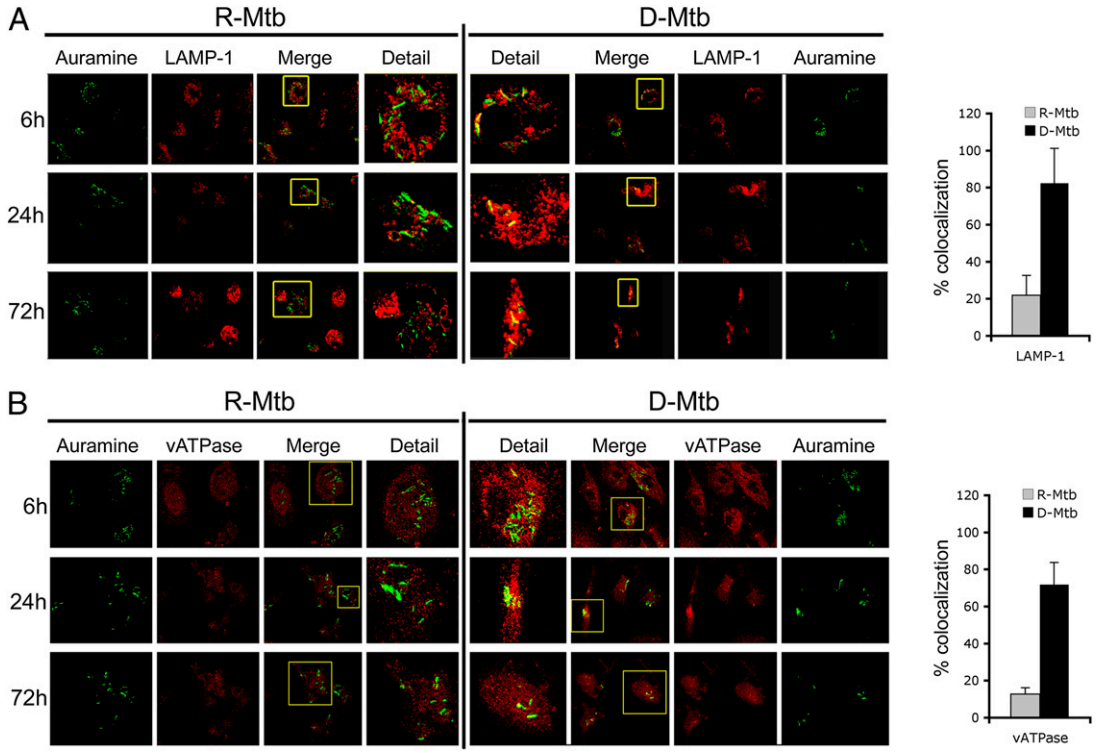

FIGURE 4. Different intracellular localization of D-Mtb or R-Mtb in infected macrophages. (**A**) Macrophages infected o/n with D-Mtb or R-Mtb were fixed at indicated time points and stained with auramine (green) and with anti–LAMP-1 mAb (red) and then examined by confocal microscopy (original magnification ×600, inset ×1800). R-Mtb was rarely found in LAMP-1$^+$ compartments, whereas most D-Mtb colocalized with the phagosomal marker LAMP-1 (yellow on image merging). The histogram shows the percentage of mycobacteria colocalizing with LAMP-1 at 24 h infection. Data represent means ± SEM of three independent experiments. (**B**) vATPase is not excluded in intracellular compartments of infected macrophages containing D-Mtb. Macrophages infected o/n with D-Mtb or R-Mtb were fixed at indicated time points and stained with auramine (green) and with anti-vATPase mAb (red) and then examined by confocal microscopy (original magnification ×600, inset ×1800). R-Mtb cells were rarely found in vATPase$^+$ compartments, whereas an increasing number of D-Mtb colocalized with vATPase in the same intracellular compartments (yellow spots on image merging) in the examined time frame. One representative experiment out of three is shown. The histogram shows the percentage of mycobacteria colocalizing with vATPase at 24 h infection. Data represent means ± SEM of three independent experiments.

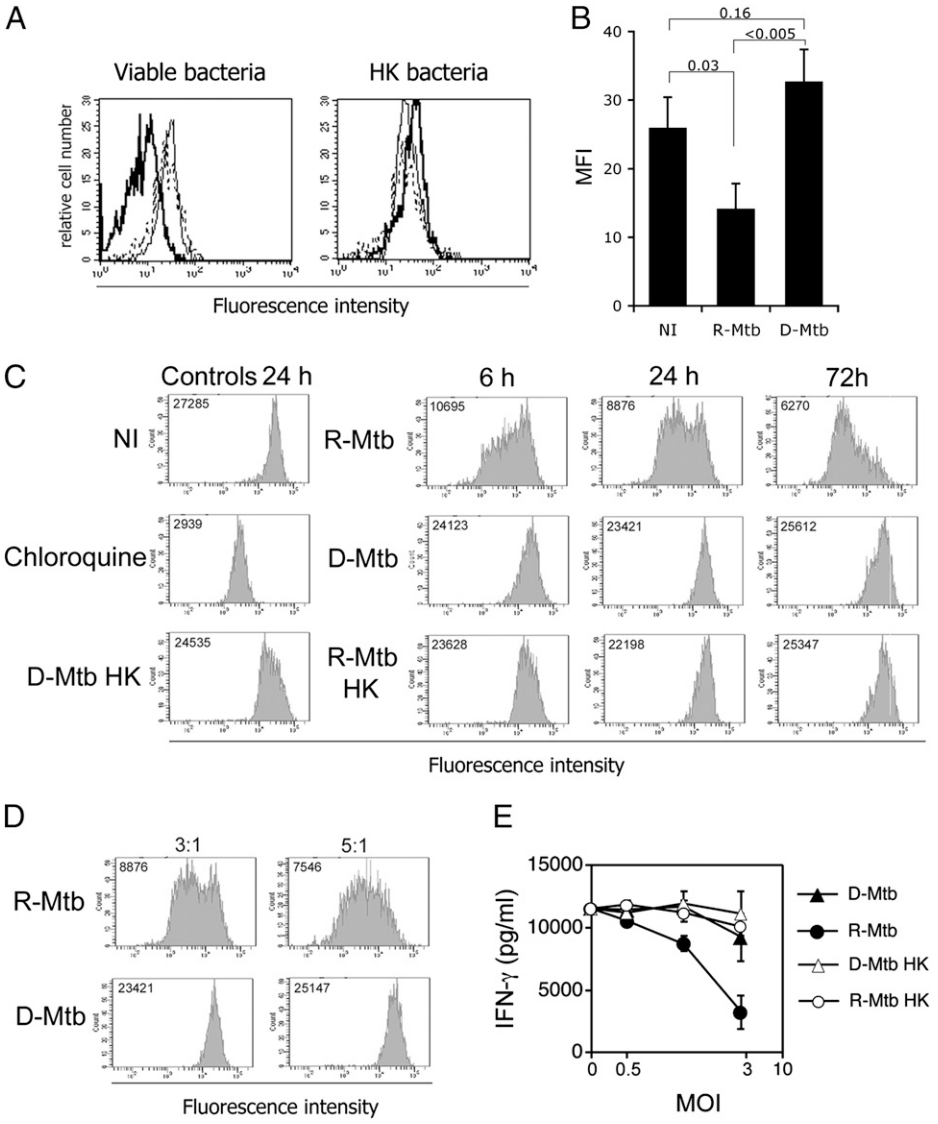

FIGURE 5. The acidic intracellular compartments do not vary in infected macrophages containing D-Mtb, which does not block the proteolytic capacity of infected macrophages to digest proteins. (**A**) Measure of the phagosome acidification in terms of fluorescence intensity of the acidotropic acid dye LysoTracker Red in macrophages after 48 h infection with D-Mtb or R-Mtb or treatment with HK bacteria by flow cytometry. Broken line indicates noninfected macrophages, solid line indicates macrophages infected with D-Mtb, and bold line indicates macrophages infected with R-Mtb. One representative experiment out of three is shown. (**B**) Mean fluorescence intensity (MFI) ± SEM of LysoTracker Red in noninfected (NI) or D-Mtb– or R-Mtb–infected macrophages of six independent experiments. Numbers represent *p* values of the indicated differences in MFI. (**C**) Macrophages infected for 6, 24, or 72 h with D-Mtb or R-Mtb or treated with HK mycobacteria were incubated with DQ-BSA, a probe that became fluorescent when the quencher was removed by proteolytic digestion, fixed, and then analyzed for fluorescence intensity by flow cytometry. Numbers inside the plots indicate the mean intensity of fluorescence. Noninfected (NI) macrophages showed a high level of fluorescence indicating a normal proteolytic degradation of the probe DQ-BSA. Macrophages treated with chloroquine, which reduces the proteolytic degradation of proteins by increasing the phagosomal pH, showed a reduced fluorescence. Most macrophages infected with R-Mtb showed a time-dependent reduced fluorescence, indicating a low level of proteolysis induced by R-Mtb. (**D**) The reduced fluorescence of R-Mtb–infected macrophages was MOI-dependent (the MOI-dependent fluorescence of a 24-h infection is shown). Macrophages treated with HK mycobacteria or infected with D-Mtb showed a level of fluorescence similar to noninfected macrophages (C), indicating that they do not interfere with protein processing. One representative experiment out of three is shown. (**E**) Macrophages infected o/n with increasing MOIs of D-Mtb or R-Mtb or treated with increasing ratios of HK D-Mtb or R-Mtb were incubated with MP65, a *Candida albicans* recombinant protein, and then cultured with one autologous MP65-specific TCC. IFN-γ release was used as a measure of TCC activation after 48 h. Macrophages infected with D-Mtb or treated with HK mycobacteria present MP65 with efficiency similar to that of noninfected APC, whereas R-Mtb–infected macrophages show a reduced Ag presentation capacity. One experiment out of two is shown as means ± SD of triplicate wells.

We show that APC infected with D-Mtb present an increased amount of Ag in comparison with APC infected with R-Mtb. This conclusion is supported by results showing that 1) D-Mtb and R-Mtb infect macrophages with the same efficiency, 2) PPD-specific T cell clones are activated to a higher extent by macrophages and DC infected with D-Mtb in comparison with APC infected with R-Mtb, 3) D-Mtb and R-Mtb express comparable amounts of the Ags recognized by our clones, 4) D-Mtb and R-Mtb induce APC to express similar levels of stimulatory and costimulatory molecules and to secrete the same level of cytokines, and 5) R-Mtb–, but not D-Mtb–, infected macrophages are impaired in presenting not only *M. tuberculosis* Ags, but also a soluble *Candida albicans* protein to a specific autologous TCC.

R-Mtb is highly adapted to life within macrophages, and it can modulate macrophage defenses and inhibit the processing of its Ags for the MHC class II pathway to promote its intracellular survival (32, 33). In particular, metabolically active *M. tuberculosis* is endowed with the capacity to arrest phagosomal maturation (34–37). To find a possible explanation for the increased Ag presentation capacity of D-Mtb–infected macrophages, we tested whether D-Mtb shares with R-Mtb the same ability to arrest phagosomal maturation (38). Phagosome maturation is a highly complex process in which phagosomes harboring engulfed particles interact with other intracellular organelles and get acidified (39) by proton pump vATPase polymerization that reduces the neutral pH to an acidic pH (40). Our results show that following infection of macrophages, D-Mtb reaches intracellular compartments where it colocalizes with the mature phagosome markers LAMP-1 and vATPase. Moreover, D-Mtb–infected macrophages maintain their capacity to digest proteins in acidic compartments differently from R-Mtb–infected macrophages. These results indicate that D-Mtb is not endowed with the ability to arrest the phagosome maturation that characterizes R-Mtb, showing in this respect analogy with HK *M. tuberculosis*, BCG, and other *M. tuberculosis* mutant strains (41).

An important difference with *M. tuberculosis* that makes BCG an attenuated vaccine strain resides in its lack of the region of difference-1. Region of difference-1 is part of a 15-gene locus known as ESX-1 that encodes a specialized secretion system dedicated to the secretion of CFP-10 and ESAT-6 (42). Interestingly, following infection of DC, the Mtb strain lacking ESAT-6 and CFP-10 localized to LAMP-1$^+$ phagolysomes (43), suggesting the pivotal role of these proteins in the inhibition of phagosome maturation. In addition to products of the ESX-1 gene, *M. tuberculosis* uses a range of lipids, such as lipoarabinomannan, and protein effectors to alter the phosphatidylinositol 3-phosphate signaling (44, 45) involved in phagosome maturation. In particular, *M. tuberculosis* produces the phosphatase SapM, which specifically hydrolyses phosphatidylinositol 3-phosphate (35). We show that D-Mtb downmodulates expression of the *esat6* gene, suggesting that in dormancy *M. tuberculosis* secretes reduced amounts of ESAT-6 in comparison with R-Mtb. Moreover, expression of the gene *Rv3309c*, which encodes for SapM, was previously found downregulated in D-Mtb obtained with the same Wayne culture method we used and in stressed mouse macrophages (46). Taken together, these data are highly suggestive for the pivotal role played by the reduced expression of *esat6* and *SapM* as a possible mechanism used by D-Mtb to permit phagosome maturation and downstream events leading to an increased Ag processing and presentation to specific CD4$^+$ T lymphocytes.

D-Mtb is currently thought to represent the mycobacterial stage that resists eradication and persists in LTBI (4, 47). In this light, it may be considered unexpected that D-Mtb is recognized by T lymphocytes with higher efficiency than R-Mtb. Because the *M. tuberculosis*–specific T lymphocytes that expanded during primary infection still persist in LTBI, our results would favor the hypothesis that D-Mtb is easily killed by host macrophages upon specific T cell help (48). This apparent incoherence may be explained considering that it is highly improbable that D-Mtb could infect tissue macrophages in LTBI, as dormant bacteria do not replicate and cannot invade host cells unless they resuscitate as "scout mycobacteria" to sense the environment, but in this case they would lose the characteristics of dormant bacteria (4, 47). Even though the physical location of bacilli during LTBI remains poorly understood (9, 49, 50), it is conceivable that dormant bacteria reside in cells, which have a scarce ability to act as APC, but behave as an *M. tuberculosis* reservoir instead. It may be thought that R-Mtb shifts to dormancy within infected macrophages after having subverted their antimicrobial and APC potential (11). Additionally, *M. tuberculosis* may reside within subverted or foamy macrophages in mature granulomas (51, 52), where T cells are physically separated from infected cells by a fibrous wall or caseum that limits APC/lymphocyte interactions (4). Lastly, *M. tuberculosis* may rest dormant in non-APC, representing sites of immunoprivilege (14) for *M. tuberculosis* persistence in LTBI.

Recent findings indicate that bacteria with features of dormant, lipid body–positive *M. tuberculosis* cells are found in sputa from patients with active TB with frequencies ranging from 3 to 86% (19). Because bacteria in sputa reasonably reflect the population of *M. tuberculosis* in active pulmonary foci, these findings indicate that a large population of D-Mtb is present in active TB lesions. Irrespective of the stimuli that force *M. tuberculosis* to switch to a dormant phenotype, it follows that during active TB the immune system is faced not only with R-Mtb, but also with D-Mtb. Therefore, our in vitro model fits with the in vivo scenario of active TB, where replicating, dormant, or both stages of *M. tuberculosis* challenge the immune system. This model suggests that D-Mtb may represent the form of *M. tuberculosis* that mainly contributes to the stimulation host-specific immune response in TB.

The immune response in TB is extremely complex (53), and factors driving the double role of the acquired immunity in protecting against *M. tuberculosis* or in causing the tissue damage are not yet completely understood (54–56). We may suppose that the evolution of a "double personality" would allow *M. tuberculosis* in its replicative form to escape from immunosurveillance to outgrow and colonize, but also to induce a strong immune response that contributes to tissue damage, shifting to dormancy. In fact, cavitation and damage of lung tissue and bronchi caused by immunopathology are necessary for *M. tuberculosis* to gain access to the environment and to be transmitted to susceptible individuals (10).

As a final consideration, the variable relative frequency of D-Mtb and R-Mtb found in sputa may also mirror the population of *M. tuberculosis* present in infecting droplets released by patients with open TB lesions (19). Accordingly, the outcome of a primary infection would be probably different in dependence of both the number of mycobacteria and the relative frequency of D-Mtb and R-Mtb in infecting droplets. Interesting in this view is our observation indicating that DC, which are considered the APC involved in the priming of Ag-specific T cells, when infected by D-Mtb undergo maturation and present a higher amount of Ag than do R-Mtb–infected DC.

In conclusion, the capacity of Mtb to switch to a nonreplicating form of dormancy may represent not only a mechanism of survival in hostile environmental conditions, but also a strategy to modulate and subjugate the host adaptive immune system in the different stages of TB.

Acknowledgments

We thank Lanfranco Fattorini for suggestions regarding the culture method to obtain dormant *M. tuberculosis*, and Roberto La Valle and Silvia Sandini for providing recombinant MP65. We also thank Gennaro De Libero and Vincenzo Barnaba for discussions and Maurice Di Santolo for English revision of the manuscript.

Disclosures

The authors have no financial conflicts of interest.

References

1. Connell, D. W., M. Berry, G. Cooke, and O. M. Kon. 2011. Update on tuberculosis: TB in the early 21st century. *Eur. Respir. Rev.* 20: 71–84.

2. Tufariello, J. M., J. Chan, and J. L. Flynn. 2003. Latent tuberculosis: mechanisms of host and bacillus that contribute to persistent infection. *Lancet Infect. Dis.* 3: 578–590.
3. Barry, C. E., III, H. I. Boshoff, V. Dartois, T. Dick, S. Ehrt, J. Flynn, D. Schnappinger, R. J. Wilkinson, and D. Young. 2009. The spectrum of latent tuberculosis: rethinking the biology and intervention strategies. *Nat. Rev. Microbiol.* 7: 845–855.
4. Gengenbacher, M., and S. H. Kaufmann. 2012. *Mycobacterium tuberculosis*: success through dormancy. *FEMS Microbiol. Rev.* 36: 514–532.
5. Dye, C. 2006. Global epidemiology of tuberculosis. *Lancet* 367: 938–940.
6. Jolobe, O. M. 2007. Anti-TNFα treatment and reactivation of latent tuberculosis. *Lancet* 370: 27–28.
7. Tiemersma, E. W., M. J. van der Werf, M. W. Borgdorff, B. G. Williams, and N. J. Nagelkerke. 2011. Natural history of tuberculosis: duration and fatality of untreated pulmonary tuberculosis in HIV negative patients: a systematic review. *PLoS ONE* 6: e17601.
8. Boussiotis, V. A., E. Y. Tsai, E. J. Yunis, S. Thim, J. C. Delgado, C. C. Dascher, A. Berezovskaya, D. Rousset, J. M. Reynes, and A. E. Goldfeld. 2000. IL-10-producing T cells suppress immune responses in anergic tuberculosis patients. *J. Clin. Invest.* 105: 1317–1325.
9. Ramakrishnan, L. 2012. Revisiting the role of the granuloma in tuberculosis. *Nat. Rev. Immunol.* 12: 352–366.
10. Cardona, P. J. 2011. A spotlight on liquefaction: evidence from clinical settings and experimental models in tuberculosis. *Clin. Dev. Immunol.* 2011: 868246.
11. Baena, A., and S. A. Porcelli. 2009. Evasion and subversion of antigen presentation by *Mycobacterium tuberculosis. Tissue Antigens* 74: 189–204.
12. Meena, L. S., and Rajni. 2010. Survival mechanisms of pathogenic *Mycobacterium tuberculosis* H37Rv. *FEBS J.* 277: 2416–2427.
13. Neyrolles, O., R. Hernández-Pando, F. Pietri-Rouxel, P. Fornès, L. Tailleux, J. A. Barrios Payán, E. Pivert, Y. Bordat, D. Aguilar, M. C. Prévost, et al. 2006. Is adipose tissue a place for *Mycobacterium tuberculosis* persistence? *PLoS ONE* 1: e43.
14. Hernández-Pando, R., M. Jeyanathan, G. Mengistu, D. Aguilar, H. Orozco, M. Harboe, G. A. Rook, and G. Bjune. 2000. Persistence of DNA from *Mycobacterium tuberculosis* in superficially normal lung tissue during latent infection. *Lancet* 356: 2133–2138.
15. Hampshire, T., S. Soneji, J. Bacon, B. W. James, J. Hinds, K. Laing, R. A. Stabler, P. D. Marsh, and P. D. Butcher. 2004. Stationary phase gene expression of *Mycobacterium tuberculosis* following a progressive nutrient depletion: a model for persistent organisms? *Tuberculosis (Edinb.)* 84: 228–238.
16. Wayne, L. G., and L. G. Hayes. 1998. Nitrate reduction as a marker for hypoxic shiftdown of Mycobacterium tuberculosis. *Tuber. Lung Dis.* 79: 127–132.
17. Voskuil, M. I., K. C. Visconti, and G. K. Schoolnik. 2004. *Mycobacterium tuberculosis* gene expression during adaptation to stationary phase and low-oxygen dormancy. *Tuberculosis (Edinb.)* 84: 218–227.
18. Deb, C., C. M. Lee, V. S. Dubey, J. Daniel, B. Abomoelak, T. D. Sirakova, S. Pawar, L. Rogers, and P. E. Kolattukudy. 2009. A novel in vitro multiple-stress dormancy model for *Mycobacterium tuberculosis* generates a lipid-loaded, drug-tolerant, dormant pathogen. *PLoS ONE* 4: e6077.
19. Garton, N. J., S. J. Waddell, A. L. Sherratt, S. M. Lee, R. J. Smith, C. Senner, J. Hinds, K. Rajakumar, R. A. Adegbola, G. S. Besra, et al. 2008. Cytological and transcript analyses reveal fat and lazy persister-like bacilli in tuberculous sputum. *PLoS Med.* 5: e75.
20. Mukamolova, G. V., O. Turapov, J. Malkin, G. Woltmann, and M. R. Barer. 2010. Resuscitation-promoting factors reveal an occult population of tubercle Bacilli in Sputum. *Am. J. Respir. Crit. Care Med.* 181: 174–180.
21. Iona, E., M. Pardini, M. C. Gagliardi, M. Colone, A. R. Stringaro, R. Teloni, L. Brunori, R. Nisini, L. Fattorini, and F. Giannoni. 2012. Infection of human THP-1 cells with dormant Mycobacterium tuberculosis. *Microbes Infect.* 14: 959–967.
22. Wayne, L. G., ed. 2001. *In Vitro Model of Hypoxically Induced Nonreplicating Persistence of* Mycobacterium tuberculosis. Humana Press, Totowa, NJ.
23. Wayne, L. G., and L. G. Hayes. 1996. An in vitro model for sequential study of shiftdown of *Mycobacterium tuberculosis* through two stages of nonreplicating persistence. *Infect. Immun.* 64: 2062–2069.
24. Mariotti, S., V. Sargentini, C. Marcantonio, E. Todero, R. Teloni, M. C. Gagliardi, A. R. Ciccaglione, and R. Nisini. 2008. T-cell-mediated and antigen-dependent differentiation of human monocyte into different dendritic cell subsets: a feedback control of Th1/Th2 responses. *FASEB J.* 22: 3370–3379.
25. Nisini, R., G. Romagnoli, M. J. Gomez, R. La Valle, A. Torosantucci, S. Mariotti, R. Teloni, and A. Cassone. 2001. Antigenic properties and processing requirements of 65-kilodalton mannoprotein, a major antigen target of anti-*Candida* human T-cell response, as disclosed by specific human T-cell clones. *Infect. Immun.* 69: 3728–3736.
26. Desjardin, L. E., L. G. Hayes, C. D. Sohaskey, L. G. Wayne, and K. D. Eisenach. 2001. Microaerophilic induction of the α-crystallin chaperone protein homologue (*hspX*) mRNA of *Mycobacterium tuberculosis. J. Bacteriol.* 183: 5311–5316.
27. Sturgill-Koszycki, S., P. H. Schlesinger, P. Chakraborty, P. L. Haddix, H. L. Collins, A. K. Fok, R. D. Allen, S. L. Gluck, J. Heuser, and D. G. Russell. 1994. Lack of acidification in *Mycobacterium* phagosomes produced by exclusion of the vesicular proton-ATPase. *Science* 263: 678–681.
28. Singh, C. R., R. A. Moulton, L. Y. Armitige, A. Bidani, M. Snuggs, S. Dhandayuthapani, R. L. Hunter, and C. Jagannath. 2006. Processing and presentation of a mycobacterial antigen 85B epitope by murine macrophages is dependent on the phagosomal acquisition of vacuolar proton ATPase and in situ activation of cathepsin D. *J. Immunol.* 177: 3250–3259.
29. Via, L. E., R. A. Fratti, M. McFalone, E. Pagan-Ramos, D. Deretic, and V. Deretic. 1998. Effects of cytokines on mycobacterial phagosome maturation. *J. Cell Sci.* 111: 897–905.
30. Eswarappa, S. M., V. D. Negi, S. Chakraborty, B. K. Chandrasekhar Sagar, and D. Chakravortty. 2010. Division of the *Salmonella*-containing vacuole and depletion of acidic lysosomes in *Salmonella*-infected host cells are novel strategies of *Salmonella enterica* to avoid lysosomes. *Infect. Immun.* 78: 68–79.
31. La Valle, R., S. Sandini, M. J. Gomez, F. Mondello, G. Romagnoli, R. Nisini, and A. Cassone. 2000. Generation of a recombinant 65-kilodalton mannoprotein, a major antigen target of cell-mediated immune response to *Candida albicans. Infect. Immun.* 68: 6777–6784.
32. Pethe, K., D. L. Swenson, S. Alonso, J. Anderson, C. Wang, and D. G. Russell. 2004. Isolation of *Mycobacterium tuberculosis* mutants defective in the arrest of phagosome maturation. *Proc. Natl. Acad. Sci. USA* 101: 13642–13647.
33. Vandal, O. H., L. M. Pierini, D. Schnappinger, C. F. Nathan, and S. Ehrt. 2008. A membrane protein preserves intrabacterial pH in intraphagosomal *Mycobacterium tuberculosis. Nat. Med.* 14: 849–854.
34. Flannagan, R. S., G. Cosío, and S. Grinstein. 2009. Antimicrobial mechanisms of phagocytes and bacterial evasion strategies. *Nat. Rev. Microbiol.* 7: 355–366.
35. Vergne, I., J. Chua, H. H. Lee, M. Lucas, J. Belisle, and V. Deretic. 2005. Mechanism of phagolysosome biogenesis block by viable *Mycobacterium tuberculosis. Proc. Natl. Acad. Sci. USA* 102: 4033–4038.
36. Walburger, A., A. Koul, G. Ferrari, L. Nguyen, C. Prescianotto-Baschong, K. Huygen, B. Klebl, C. Thompson, G. Bacher, and J. Pieters. 2004. Protein kinase G from pathogenic mycobacteria promotes survival within macrophages. *Science* 304: 1800–1804.
37. Russell, D. G., B. C. Vanderven, S. Glennie, H. Mwandumba, and R. S. Heyderman. 2009. The macrophage marches on its phagosome: dynamic assays of phagosome function. *Nat. Rev. Immunol.* 9: 594–600.
38. Lee, B. Y., D. L. Clemens, and M. A. Horwitz. 2008. The metabolic activity of *Mycobacterium tuberculosis*, assessed by use of a novel inducible GFP expression system, correlates with its capacity to inhibit phagosomal maturation and acidification in human macrophages. *Mol. Microbiol.* 68: 1047–1060.
39. Desjardins, M., L. A. Huber, R. G. Parton, and G. Griffiths. 1994. Biogenesis of phagolysosomes proceeds through a sequential series of interactions with the endocytic apparatus. *J. Cell Biol.* 124: 677–688.
40. Yates, R. M., A. Hermetter, and D. G. Russell. 2005. The kinetics of phagosome maturation as a function of phagosome/lysosome fusion and acquisition of hydrolytic activity. *Traffic* 6: 413–420.
41. Guinn, K. M., M. J. Hickey, S. K. Mathur, K. L. Zakel, J. E. Grotzke, D. M. Lewinsohn, S. Smith, and D. R. Sherman. 2004. Individual RD1-region genes are required for export of ESAT-6/CFP-10 and for virulence of *Mycobacterium tuberculosis. Mol. Microbiol.* 51: 359–370.
42. Simeone, R., D. Bottai, and R. Brosch. 2009. ESX/type VII secretion systems and their role in host-pathogen interaction. *Curr. Opin. Microbiol.* 12: 4–10.
43. van der Wel, N., D. Hava, D. Houben, D. Fluitsma, M. van Zon, J. Pierson, M. Brenner, and P. J. Peters. 2007. *M. tuberculosis* and *M. leprae* translocate from the phagolysosome to the cytosol in myeloid cells. *Cell* 129: 1287–1298.
44. Vieira, O. V., R. J. Botelho, L. Rameh, S. M. Brachmann, T. Matsuo, H. W. Davidson, A. Schreiber, J. M. Backer, L. C. Cantley, and S. Grinstein. 2001. Distinct roles of class I and class III phosphatidylinositol 3-kinases in phagosome formation and maturation. *J. Cell Biol.* 155: 19–25.
45. Fratti, R. A., J. M. Backer, J. Gruenberg, S. Corvera, and V. Deretic. 2001. Role of phosphatidylinositol 3-kinase and Rab5 effectors in phagosomal biogenesis and mycobacterial phagosome maturation arrest. *J. Cell Biol.* 154: 631–644.
46. Murphy, D. J., and J. R. Brown. 2007. Identification of gene targets against dormant phase *Mycobacterium tuberculosis* infections. *BMC Infect. Dis.* 7: 84.
47. Chao, M. C., and E. J. Rubin. 2010. Letting sleeping dos lie: does dormancy play a role in tuberculosis? *Annu. Rev. Microbiol.* 64: 293–311.
48. Flynn, J. L., J. Chan, K. J. Triebold, D. K. Dalton, T. A. Stewart, and B. R. Bloom. 1993. An essential role for interferon γ in resistance to *Mycobacterium tuberculosis* infection. *J. Exp. Med.* 178: 2249–2254.
49. van Crevel, R., T. H. Ottenhoff, and J. W. van der Meer. 2002. Innate immunity to *Mycobacterium tuberculosis. Clin. Microbiol. Rev.* 15: 294–309.
50. Gideon, H. P., and J. L. Flynn. 2011. Latent tuberculosis: what the host "sees"? *Immunol. Res.* 50: 202–212.
51. Ehlers, S. 2009. Lazy, dynamic or minimally recrudescent? On the elusive nature and location of the *mycobacterium* responsible for latent tuberculosis. *Infection* 37: 87–95.
52. Peyron, P., J. Vaubourgeix, Y. Poquet, F. Levillain, C. Botanch, F. Bardou, M. Daffé, J. F. Emile, B. Marchou, P. J. Cardona, et al. 2008. Foamy macrophages from tuberculous patients' granulomas constitute a nutrient-rich reservoir for *M. tuberculosis* persistence. *PLoS Pathog.* 4: e1000204.
53. Ernst, J. D. 2012. The immunological life cycle of tuberculosis. *Nat. Rev. Immunol.* 12: 581–591.
54. Dorhoi, A., S. T. Reece, and S. H. Kaufmann. 2011. For better or for worse: the immune response against *Mycobacterium tuberculosis* balances pathology and protection. *Immunol. Rev.* 240: 235–251.
55. Garlanda, C., D. Di Liberto, A. Vecchi, M. P. La Manna, C. Buracchi, N. Caccamo, A. Salerno, F. Dieli, and A. Mantovani. 2007. Damping excessive inflammation and tissue damage in *Mycobacterium tuberculosis* infection by Toll IL-1 receptor 8/single Ig IL-1-related receptor, a negative regulator of IL-1/TLR signaling. *J. Immunol.* 179: 3119–3125.
56. Orme, I. M. 1998. The immunopathogenesis of tuberculosis: a new working hypothesis. *Trends Microbiol.* 6: 94–97.